Phonon-assisted intersubband transitions in wurtzite $GaN/In_xGa_{1-x}N$ quantum wells*

Zhu Jun(朱 俊)[a], Ban Shi-Liang(班士良)[a]†, and Ha Si-Hua(哈斯花)[b]

[a] *Key Laboratory of Semiconductor Photovoltaic Technology, School of Physical Science and Technology, Inner Mongolia University, Hohhot* 010021, *China*

[b] *Department of Physics, College of Sciences, Inner Mongolia University of Technology, Hohhot* 010051, *China*

(Received 2 January 2012; revised manuscript received 21 March 2012)

A detailed numerical calculation on the phonon-assisted intersubband transition rates of electrons in wurtzite $GaN/In_xGa_{1-x}N$ quantum wells is presented. The quantum-confined Stark effect induced by the built-in electric field and the ternary mixed crystal effect are considered. The electron states are obtained by iteratively solving the coupled Schrödinger and Poisson equations and the dispersion property of each type of phonon modes is considered in the derivation of Fermi's golden rule to evaluate the transition rates. It is indicated that the interface and half-space phonon scattering play an important role in the process of 1–2 radiative transition. The transition rate is also greatly reduced by the built-in electric field. The present work can be helpful for the structural design and simulation of new semiconductor lasers.

Keywords: phonon-assisted intersubband transition, wurtzite quantum well, built-in electric field

PACS: 73.21.Fg, 72.10.Di, 77.65.Ly **DOI:** 10.1088/1674-1056/21/9/097301

1. Introduction

The electron-phonon (e–p) interaction plays a dominant role in determining the radiative intersubband transition and fast carrier relaxation for semiconductor lasers, such as tunneling injection lasers and quantum cascade lasers.[1−5] Based on the Fermi's golden rule, the optical phonon scattering rates for intersubband transitions between quasi-bound states in single quantum wells (QWs),[6,7] step QWs,[8,9] double QWs (DQWs),[10−12] and multiple QWs[13−15] have been studied during the last two decades, respectively. It has been demonstrated that the transition rates can be modulated for potential device applications by structural optimization. However, the optical phonon modes in hetero-structures usually including interface (IF), confined (CO), and half-space (HS) modes have not been considered thoroughly in these works except Refs. [9] and [10]. Many authors only focused their attention on the scattering between electrons and IF phonons (or IF and CO phonons). Furthermore, the dispersive properties of optical phonons were neglected to deal with the delta functions which ensure the energy and momentum conservation. Although the k-dependent phonon energy was involved, the angle between the initial and final momentum was not taken into account in Ref. [6]. The scattering rates were also investigated using the Green's function formalism by considering the influence of two-dimensional electron gas (2DEG).[16,17] However, the leading-order electron self-energy was obtained under the bulk-phonon approximation.

Unfortunately, these works mentioned above were only limited to the traditional zinc–blende structures. As for wurtzite semiconductor heterostructures, lower symmetry crystal structure and residual strain in the epilayers cause a strong built-in electric field (BEF) induced by the spontaneous and piezoelectric polarization to accumulate high-density 2DEG near heterointerfaces.[18−20] Phonon modes and the corresponding e–p interaction in wurtzite QWs are quite different from that in zinc–blende QWs due to the anisotropy of a wurtzite structure. It was found that there may be four distinct classes of optical phonon modes, i.e., IF, CO, HS, and propagating (PR) modes, and they may transform mutually with increasing composition in wurtzite multiple-layer structures consisting of ternary mixed crystal (TMC).[20,21] All types

*Project supported by the National Natural Science Foundation of China (Grant No. 60966001) and the Science Foundation of Inner Mongolia Autonomous Region, China (Grant No. 2010BS0102).

†Corresponding author. E-mail: slban@imu.edu.cn

© 2012 Chinese Physical Society and IOP Publishing Ltd

of phonons are dispersive and the corresponding e–p interaction Hamiltonians are very complicated.[20−26] These peculiar properties have a significant impact on the intersubband scattering in wurtzite heterostructures. Park *et al.*[27] and Pokatilov *et al.*[28] showed the polarization effect on the transition rates in wurtzite QWs consisting of nitrides compounds. However, the former authors neglected the specific optical phonon modes in their calculation and the latter ones only discussed the acoustic phonon scattering. Without considering the BEF effect, the transition rates due to the scattering of the electron and the IF and CO optical phonons were investigated in wurtzite QWs by Komirenko *et al.*[29] and in wurtzite DQWs by Lü and Cao.[30] Their results suggested that the scattering rates are greatly influenced by the quantization and dispersion of phonon modes. However, few works have systemically studied the optical phonon modes in wurtzite QWs consisting of a TMC (e.g., $In_xGa_{1-x}N$) and the effects of the BEF and 2DEG on the corresponding e–p scattering are still unclear.

In this paper, we present a detailed investigation on the phonon scattering rates for intersubband transitions between the ground state and the first excited states in wurtzite GaN/In_xGa_{1-x}N QWs. The electron states are obtained by iteratively solving the coupled Schrödinger and Poisson equations and the frequency dispersion of each type of phonon modes including the TMC effect is taken into account in the derivation of Fermi's golden rule to evaluate the transition rates.

2. Electron states in wurtzite GaN/In_xGa_{1-x}N QWs

Let us consider a wurtzite GaN/In_xGa_{1-x}N QW. In this structure, the z-axis is taken to be parallel to the hexagonal reference c axis, which is oriented along the direction of the crystal growth. The well material $In_xGa_{1-x}N$ locates between $z = \pm d_w/2$, while the barrier material GaN fills up the region $d_w/2 < |z| < d_w/2 + d_b$, where d_w and d_b denote the well and barrier widths, respectively. The electron states take the form

$$|n, \boldsymbol{k}_\perp\rangle = \psi(\boldsymbol{k}_\perp, z) = \frac{1}{\sqrt{A}} \mathrm{e}^{\mathrm{i}\boldsymbol{k}_\perp \cdot \boldsymbol{\rho}} \varphi_n(z), \tag{1}$$

which includes a free in-plane wave function with interface area A and wave vector $\boldsymbol{k}_\perp$, as well as a confined wave function in the z direction. Within the framework of the effective mass approximation, the Schrödinger equation in the z direction for a confined electron with charge e is given by

$$\left\{ -\frac{\hbar^2}{2}\frac{\partial}{\partial z}\left[\frac{1}{m_z(z)}\right]\frac{\partial}{\partial z} + V(z) + eF(z)z + V_{\mathrm{H}}(z) + V_{\mathrm{xc}}(z)\right\}\varphi_n(z) = E_n\varphi_n(z), \tag{2}$$

where V_{H} is the Hartree electrostatic potential, and V_{xc} is the exchange-correlation potential. In the above equation, $m_z(z)$ is the position-dependent effective mass of the electron, $V(z)$ is the height of potential barriers, the ratio of the conduction band to the valence band offset has been assumed to be 75:25. The $F(z)$ is the BEF which can be expressed by

$$F(z) = \begin{cases} F_{\mathrm{w}}, & |z| \le d_{\mathrm{w}}/2, \\ F_{\mathrm{b}}, & d_{\mathrm{w}}/2 < |z| < d_{\mathrm{w}}/2 + d_{\mathrm{b}}\ . \end{cases} \tag{3}$$

with the BEF in each layer given by[18]

$$F_{\mathrm{w}} = \frac{d_{\mathrm{b}}(P_{\mathrm{b}}^{\mathrm{sp}} + P_{\mathrm{b}}^{\mathrm{pz}} - P_{\mathrm{w}}^{\mathrm{sp}} - P_{\mathrm{w}}^{\mathrm{pz}})}{d_{\mathrm{b}}\varepsilon_{0\mathrm{w}} + d_{\mathrm{w}}\varepsilon_{0\mathrm{b}}}, \tag{4}$$

and

$$F_{\mathrm{b}} = -\frac{d_{\mathrm{w}}}{d_{\mathrm{b}}}F_{\mathrm{w}}. \tag{5}$$

Here, $P_j^{\mathrm{sp}}$and $P_j^{\mathrm{pz}}$are the spontaneous and piezoelectric polarization of layer $j(j$ =b,w), ε_{0j} is the static dielectric constant, and P_j^{pz} can be written as[31]

$$P_j^{\mathrm{pz}} = 2\varepsilon_{xx,j}\left(e_{31,j} - e_{33,j}\frac{c_{13,j}}{c_{33,j}}\right), \tag{6}$$

where $e_{31,j}$ and $e_{33,j}$ are the piezoelectric constants, $c_{13,j}$ and $c_{33,j}$ are the elastic constants, and the strain tensor components can be given by[32]

$$\varepsilon_{xx,j} = \varepsilon_{yy,j} = \frac{a_{\mathrm{eq}} - a_j}{a_j}, \tag{7}$$

where a_{eq} is the equilibrium lattice constant shared by all layers, which can be written as

$$a_{\mathrm{eq}} = \frac{a_{\mathrm{w}}d_{\mathrm{w}} + a_{\mathrm{b}}d_{\mathrm{b}}}{d_{\mathrm{w}} + d_{\mathrm{b}}}. \tag{8}$$

According to the Poisson equation, the Hartree electrostatic potential $V_{\mathrm{H}}(z)$ can be determined by

$$\frac{\mathrm{d}}{\mathrm{d}z}\left[\varepsilon_0(z)\frac{\mathrm{d}}{\mathrm{d}z}V_{\mathrm{H}}(z)\right] = -e^2[N_{\mathrm{D}}^+(z) - N(z)], \tag{9}$$

with

$$N_{\mathrm{D}}^+(z) = \frac{N_{\mathrm{D}}}{1 + 2\exp\left[\dfrac{E_{\mathrm{F}} - E_{\mathrm{D}}(z)}{k_{\mathrm{B}}T}\right]}, \tag{10}$$

and

$$N(z) = \sum_n \frac{m_z(z)k_{\rm B}T}{\pi\hbar^2}\left|\varphi_n(z)\right|^2 \times \ln\left[1+\exp\left(\frac{E_{\rm F}-E_n}{k_{\rm B}T}\right)\right], \quad (11)$$

where $\varepsilon_0(z)$ is the position-dependent static dielectric constant $N_{\rm D}$ is the donor density $E_{\rm D}$ is the donor ionization energy $k_{\rm B}$ is the Boltzmann constant, T is the temperature, and $E_{\rm F}$ is the Fermi energy which can be derived from the condition of charge neutrality

$$\int_{-\infty}^{+\infty}[N_{\rm D}^{+}(z)-N(z)]\,{\rm d}z = 0. \quad (12)$$

Using the local density approximation, the exchange-correlation potential in Eq. (2) can be formulated in an analytic form[33]

$$V_{\rm xc}(z) = \frac{e^2}{4\pi^2\varepsilon_0(z)a_{\rm B}(z)r_{\rm S}(z)}\left(\frac{9}{4}\pi\right)^{1/3} \times\left\{1+0.0545r_{\rm S}(z)\ln\left[1+\frac{11.4}{r_{\rm S}(z)}\right]\right\}, \quad (13)$$

where the effective Bohr radius is defined as $a_{\rm B}(z) = \varepsilon_0(z)\hbar^2/e^2m_z(z)$, and the radius of a sphere containing one electron as $r_{\rm S}(z) = \{(3/4\pi)[a_{\rm B}^3(z)N(z)]^{-1}\}^{1/3}$.

Therefore, the eigen energies E_n and wave functions $\varphi_n(z)$ of the confined electron can be obtained by self-consistently solving the Schrödinger equation (2) and the Poisson equation (6) via an iterative procedure.

3. Phonon-assisted intersubband transitions in wurtzite GaN/In$_x$Ga$_{1-x}$N QWs

The e–p interaction Hamiltonian can be written as

$$H_{\rm e-p} = \sum_\beta\sum_{\boldsymbol{k}}\left[e\phi_\beta(q,z)\,{\rm e}^{{\rm i}\boldsymbol{q}\cdot\boldsymbol{\rho}}a_{k\beta}+{\rm h.c.}\right], \quad (14)$$

where $a^{+}_{\boldsymbol{k}\beta}(a_{\boldsymbol{k}\beta})$ is the creation (annihilation) operator of an optical phonon with frequency $\omega_\beta(\boldsymbol{q})$ and wave vector $\boldsymbol{k} = (\boldsymbol{q},\ k_z)$. The β refers to the IF, CO, HS, and PR phonon modes, respectively. It should be pointed out that the summation over $\boldsymbol{k}$ becomes $\sum_q$ since $k_z = 0$ for IF modes, $\sum_{\boldsymbol{k}}$ becomes $\sum_{\boldsymbol{q}}\sum_{k_{1m}}$ with $k_z = k_{1m}$ for CO modes, and $\sum_{\boldsymbol{k}}$ becomes $\sum_{\boldsymbol{q}}\sum_{k_{2z}}$ with $k_z = k_{2z}$ for HS and PR modes. Because of the one-mode behavior of optical phonons in TMC In$_x$Ga$_{1-x}$N, the direction-dependent dielectric functions for the well and barrier materials can be written as

$$\varepsilon_z(\omega) = \varepsilon_\infty\frac{\omega^2-\omega_{zl}^2}{\omega^2-\omega_{zt}^2}, \quad \varepsilon_\perp(\omega) = \varepsilon_\infty\frac{\omega^2-\omega_{\perp l}^2}{\omega^2-\omega_{\perp t}^2}, \quad (15)$$

where $\omega_{z(\perp),l(t)}$ is the lattice dispersion frequency of longitudinal (transverse) optical phonon parallel (perpendicular) to the z direction. Here we assume $\varepsilon_{z,\infty} = \varepsilon_{\perp,\infty} = \varepsilon_\infty$. The phonon dispersion relations and the coupling coefficients can be obtained in the framework of the dielectric continuum model.[22,23] As shown in Ref. [14], $x = 0.056$ and $x = 0.34$ are the critical compositions for the transformation of phonon modes. All of the CO and HS phonon modes exist in the entire composition range. However, none of IF phonon modes exist when $x < 0.056$, whereas the PR modes do not exist if $x > 0.34$. Moreover, high-frequency IF phonons and low-frequency PR phonons can exist between 0.056 and 0.34. We only focus our attention on the e–p interaction from the IF, CO, and HS longitudinal-like phonon modes in the region of $0.1 < x < 1$ since the influence from the low-frequency phonons is negligibly small.

Following the Fermi's golden rule, the phonon induced transition rate of an electron from an initial state $|n,\boldsymbol{k}_\perp\rangle$ to a final state $|n',\boldsymbol{k}'_\perp\rangle$ is given by

$$W_{n,n'}(\boldsymbol{k}_\perp,\boldsymbol{k}'_\perp) = \frac{2\pi}{\hbar}\left|\langle n'\boldsymbol{k}'_\perp,N_q\pm1|\,H_{\rm e-p}\,|n\boldsymbol{k}_\perp,N_q\rangle\right|^2 \times\delta[E_{n'}+E'_\perp-E_n-E_\perp\pm\hbar\omega_\beta(\boldsymbol{q})], \quad (16)$$

where the upper and lower signs correspond to phonon absorption and emission, respectively. The delta function guarantees energy conservation in the process. $(E_{n'}-E_n)+(E'_\perp-E_\perp)\le\hbar\omega_\beta$ with $E'_\perp-E_\perp = (\hbar^2/2m_\perp)(k'^2_\perp-k^2_\perp)$ is valid for phonon absorption process even when $0 = (E_{n'}-E_n)+(E'_\perp-E_\perp)\le\hbar\omega_\beta$. In wurtzite GaN/In$_xGa_{1-x}$N QWs, $(E_{n'}-E_n)+(E'_\perp-E_\perp)$ goes far beyond the phonon energy due to a large intersubband separation between $E_{n'}$ and E_n and a large difference between $E'_\perp$ and $E_\perp$ caused by high 2DEG density (in an order of 10^{19} cm^{-2}), and therefore we will hereafter only focus on the emission process and drop the lower sign of W.

In Eq. (16), the E_n and E'_n are the band-edge energies of the n-th and n'-th subbands, $k_\perp$ and $k'_\perp$ are the in-plane electron wave vectors of the initial and final states, respectively, $E_\perp = \hbar^2k_\perp^2/2m_\perp(z)$ is

the in-plane energy, and N_q is the phonon population which can be written as

$$N_q = \frac{1}{\exp\left(\hbar\omega_\beta / k_{\rm B}T\right) - 1}. \tag{17}$$

Substituting Eqs. (1) and (14) into Eq. (16) and summing over all allowable final states, the transition rate is calculated as[15]

$$\begin{aligned} & W_{n,n'}(\boldsymbol{k}_\perp) \\ &= \sum_{\boldsymbol{k}'_\perp} W_{n,n'}(\boldsymbol{k}_\perp, \boldsymbol{k}'_\perp) \\ &= \frac{1}{4\pi^2}\frac{2\pi}{\hbar}\int_0^{2\pi} {\rm d}\theta \frac{m_\perp(z)}{\hbar^2}\left|F(q_+)\right|^2 (N_{q_+}+1) \\ &\quad \times \vartheta[E_\perp + E_n - E_{n'} - \hbar\omega_\beta(q_+)], \end{aligned} \tag{18}$$

where θ is the angle of the in-plane wave vector between the initial and final states, ϑ is the Heaviside step function, and $F(q_+)$ is defined as

$$F(q_+) = \int_{-\infty}^{+\infty} \varphi^*_{n'}(z) e\phi(q_+, z)\varphi_n(z) {\rm d}z, \tag{19}$$

where q_+ can be determined from the in-plane momentum and energy conservation laws as

$$q_+ = \sqrt{k_\perp^2 + k_\perp'^2 - 2k_\perp k'_\perp \cos\theta}, \tag{20}$$

and

$$E_{n'} - E_n + \frac{\hbar^2 k_\perp'^2}{2m_\perp(z)} - \frac{\hbar^2 k_\perp^2}{2m_\perp(z)} + \hbar\omega_\beta(q_+) = 0. \tag{21}$$

4. Numerical results and discussion

The material parameters used in our calculation are given in Table 1. Compared with that in the well region, the electron wave functions are negligibly small in barrier region beyond $4a_{\rm B}$. Hence we assumed the barrier thickness to be $4a_{\rm B}$. Here as a length unit in our numerical calculation, the Bohr radius $a_{\rm B}$ equals 2.8 nm. The donor density is taken to be 1×10^{19} cm^{-3} and temperature $T = 77$ K. Such a doping level is so high that it may cause the electron-phonon scattering to occur not only for 1-2 transition, but for 1–3 transition. Here, we do not consider 1–3 transition because higher quantized electron states can only exist in narrow QWs due to the BEF effect.

Table 1. Parameters used in the computation. The energy gaps are in units of eV, the effective masses in unites of the electron rest mass m_0, the phonon frequencies in units of cm^{-1} and the spontaneous and piezoelectric polarization in units of C/m^2 respectively.

	GaN	InN	$\rm In_xGa_{1-x}N$
$E_{\rm g}$ [a)]	3.43	0.64	$0.64x + 3.43(1-x) - 1.4x(1-x)$
$m_{{\rm e}z}$ [a)]	0.19	0.065	$0.065x + 0.19(1-x)$
$m_{{\rm e}\perp}$ [a)]	0.21	0.068	$0.068x + 0.21(1-x)$
$m_{{\rm h}z}$ [a)]	0.26	0.17	$0.17x + 0.26(1-x)$
$m_{{\rm h}\perp}$ [a)]	1.89	1.56	$1.56x + 1.89(1-x)$
ε_∞ [a)]	5.4	6.7	$6.7x + 5.4(1-x)$
ε_0 [a)]	10.18	14.7	$14.7x + 10.18(1-x)$
$\omega_{\perp{\rm l}}$ [a)]	741	593	$593x + 741(1-x)$
$\omega_{\perp{\rm t}}$ [a)]	559	476	$476x + 559(1-x)$
$\omega_{z{\rm l}}$ [a)]	734	586	$586x + 734(1-x)$
$\omega_{\perp{\rm t}}$ [a)]	532	447	$447x + 532(1-x)$
$P^{\rm sp}$ [b)]	-0.034	–0.042	$-0.042x - 0.034(1-x) + 0.037x(1-x)$
e_{31} [b)]	–0.34	–0.41	$-0.41x - 0.34(1-x)$
e_{33} [b)]	0.67	0.81	$0.81x + 0.67(1-x)$
c_{13} [b)]	103	92	$92x + 103(1-x)$
c_{33} [b)]	405	224	$224x + 405(1-x)$

[a)] Ref. [34], [b)] Ref. [31].

Figure 1 presents a schematic potential profile and wavefunction distribution of an electron at different energy levels for a typical wurtzite GaN/$\rm In_xGa_{1-x}N$ QW. It can be seen that the potential of conduction band is strongly tilted by the BEF and slightly bent due to the Hartree-Fock potential. The quantum confinement on electrons mainly comes from the triangle potential formed by the left barrier material and the well material. As a result, the electron wave functions are mostly located near the left interface and deeply

penetrate into the neighbor barrier especially for the excited states. The influence from the left barrier is more obvious than that from the right barrier.

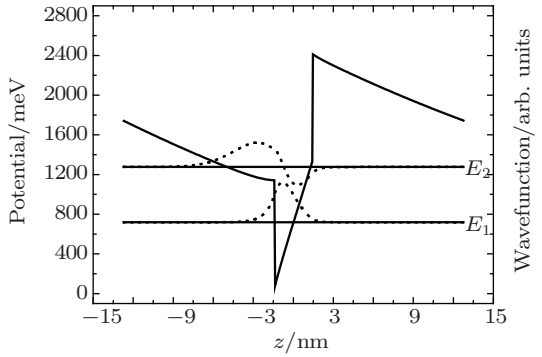


Fig. 1. Schematic potential profile and wavefunction distribution of an electron at different energy levels for a typical wurtzite GaN/$In_xGa_{1-x}N$ QW.

We plot the transition energy as a function of well width d_w in Fig. 2 and as a function of In composition x in Fig. 3. The situation without the BEF is the same as the square QW case. Meanwhile, no confined excited states exist in a quite narrow and deep QW. The variation of transition energy is only related to the quantum confinement which weakens with increasing d_w and strengthens with increasing x. Unlike the square QW case, the influence from the QW confinement is restrained by the BEF since the electron is pushed towards the left interface by the combination of BEFs in the well and in the left barrier. Moreover, according to Eqs. (4) and (5), the increase in d_w decreases the absolute value of the BEF in the well but increases it in the barrier layers, while both the BEFs in the well and in the barriers become stronger as x increases. The competition between the BEF and the QW confinement results in that the transition energy always increases with either d_w or x.

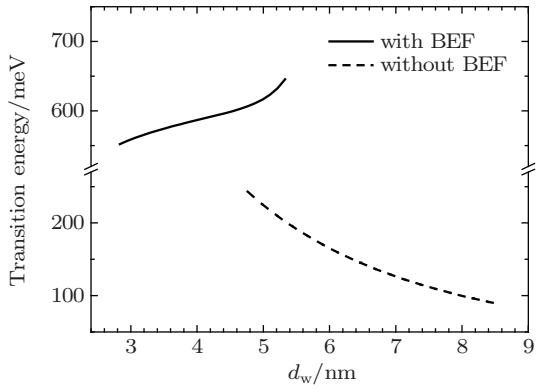


Fig. 2. Transition energy as a function of the well width d_w in GaN/$In_{0.4}Ga_{0.6}N$ QWs.

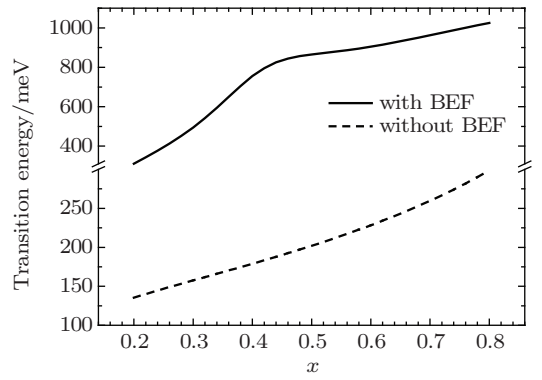


Fig. 3. Transition energy as a function of In composition x in GaN/$In_xGa_{1-x}N$ QWs with $d_w = 2a_B$.

Figure 4 illustrates the transition rate contributed by IF, CO, and HS longitudinal-like optical phonons as a function of the electron in-plane energy for a given QW with $x = 0.4$ and $d_w = 5$ nm. In this structure, the calculated transition energy is 602 meV which is larger than the phonon energy of well or barrier material. From Eq. (15), the transition rate is mainly determined by the overlap integral between the phonon potential and the electron wavefunctions. Without considering the BEF, the electron wavefunctions almost distribute in the well region and few of them penetrate into the barriers. Only the antisymmetric phonon modes contribute to the transition rate due to the wavefunction parity. The HS phonon-modes-assisted transition rate is negligible compared with the other two kinds of modes, whereas the transition rate assisted by CO phonon modes is larger than that by the IF modes. Comparatively, the BEF breaks the wavefunction symmetry and changes its distribution so that the contribution from all of the phonon modes, including the symmetric and antisymmetric ones, should be taken into account. Our results show that the transition rates assisted by the HS and IF

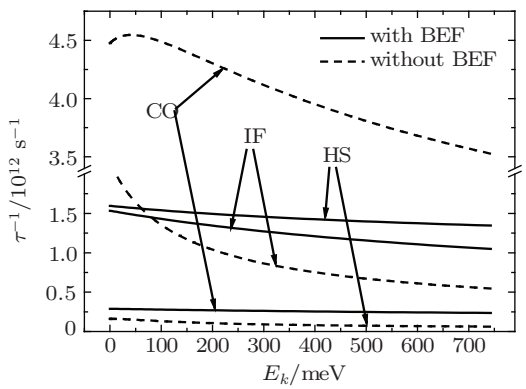


Fig. 4. Phonon-assisted intersubband transition rate contributed by IF, CO, and HS phonons as a function of the electron in-plane energy in GaN/$In_xGa_{1-x}N$ QWs with $x = 0.4$ and $d_w = 2a_B$.

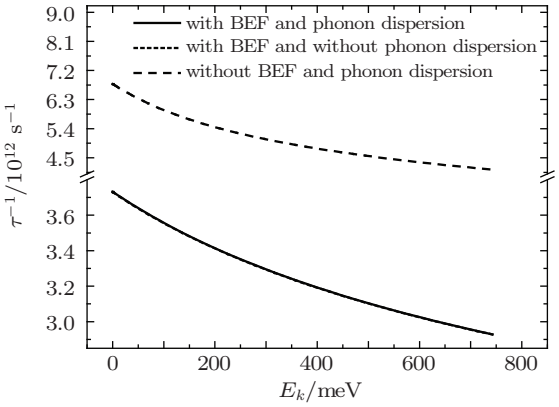


Fig. 5. Total phonon-assisted intersubband transition rate as a function of the electron in-plane energy in $GaN/In_xGa_{1-x}N$ QWs with $x = 0.4$ and $d_w = 2a_B$.

phonon modes become more important and the transition rate assisted by CO phonon is relatively small because of the BEF effect. In Fig. 5, the summation of the transition rates assisted by the three kinds of phonon modes is compared with and without a BEF. It can be found that the transition rate is obviously reduced by the BEF. However, the dispersion property of each phonon mode has little influence.

5. Conclusions

In conclusion, we have computed the phonon-assisted transition rates for intersubband transitions between the ground state and the first two excited states in wurtzite $GaN/In_xGa_{1-x}N$ QWs including the TMC effect. The quantum-confined Stark effect induced by the BEF on the electron intersubband transition and phonon scattering is discussed in detail. It is indicated that the HS and IF phonon emissions play an important role in the process of 1–2 radiative transition since the electron wavefunctions are squeezed near one of the QW interfaces and penetrate into the neighbor barrier by the BEF. The transition rate is also obviously reduced by the BEF. We believe that the present work can be helpful for the structural optimization of new semiconductor lasers. As for the case of multilayered QWs, especially step QWs, being more applicable in practice, the implanting of a nanogroove layer to the well can enhance the quantum confinement on electrons in the well region. Thereby, more energy subbands are achieved and a moderate overlap of wavefunctions between 1 and 3 subbands can be expected in these step QWs to minimize the scattering rate in the present single QWs. However, the phonon modes in multiple-layer structures consisting of ternary mixed crystals are still not very clear up to now and these problems can be discussed in future works.

References

[1] Bhattacharya P, Zhang X K, Yuan Y, Kamath K K, Klotzkin D, Caneau C and Bhat R J 1998 *Proc. SPIE* **3283** 702

[2] Bhattacharya P and Ghosh S 2002 *Appl. Phys. Lett.* **80** 3482

[3] Williams B S 2007 *Nature Photonics* **1** 517

[4] Wang F, Guo X G and Cao J C 2010 *Phys. Rev.* B **81** 045308

[5] Chen Z, Tan Z Y, Han Y J, Zhang R, Guo X G, Li H, Cao J C and Liu H C 2011 *Electron. Lett.* **47** 1002

[6] Duan W H, Zhu J L and Gu B L 1994 *Phys. Rev.* B **49** 14403

[7] Stroscio M A 1996 *J. Appl. Phys.* **80** 6864

[8] Shi J J and Pan S H 1995 *Phys. Rev.* B **51** 17681

[9] Teng H B, Sun J P, Haddad G I, Stroscio M A, Yu S G and Kim K W 1998 *J. Appl. Phys.* **84** 2155

[10] Shi J J and Pan S H 1996 *J. Appl. Phys.* **80** 3863

[11] Kisin M V, Dutta M and Stroscio M A 2002 *Int. J. High Speed Electron. Syst.* **12** 939

[12] Wu B H, Cao J C, Xia G Q and Liu H C 2003 *Eur. Phys. J.* B **33** 9

[13] Sang H Y, Gu B Y, Wang X H and Chen K Q 2005 *Phys. Lett.* A **334** 55

[14] Wang X J, Wang L L, Huang W Q, Tang L M, Zou B S and Chen K Q 2006 *Semicond. Sci. Technol.* **21** 751

[15] Gao X, Botez D and Knezevic I 2008 *J. Appl. Phys.* **103** 073101

[16] Park S H, Ahn D and Lee Y T 2000 *Jpn. J. Appl. Phys.* **39** 6601

[17] Vallone M 2002 *J. Appl. Phys.* **91** 9848

[18] Łepkowski S P, Teisseyre H, Suski T, Perlina P, Grandjean N and Massies J 2001 *Appl. Phys. Lett.* **79** 1483

[19] Teisseyre H, Suski T, Łepkowski S P, Anceau S, Perlin P, Lefebvre P, Konczewicz L, Hirayama H and Aoyagi Y 2003 *Appl. Phys. Lett.* **82** 1541

[20] Qu Y and Ban S L 2010 *Acta Phys. Sin.* **59** 4863 (in Chinese)

[21] Qu Y and Ban S L 2011 *J. Appl. Phys.* **110** 013722

[22] Komirenko S M, Kim K W, Stroscio M A and Dutta M 1999 *Phys. Rev.* B **59** 5013

[23] Lee B C, Kim K W, Stroscio M A and Dutta M 1998 *Phys. Rev.* B **58** 4860

[24] Shi J J 2003 *Phys. Rev.* B **68** 165335

[25] Shi J J, Chu X L and Goldys E M 2004 *Phys. Rev.* B **70** 115318

[26] Li L, Liu D and Shi J J 2005 *Eur. Phys. J.* B **44** 401

[27] Park S H, Ahn D and Lee Y T 2001 *Jpn. J. Appl. Phys.* **40** L941

[28] Pokatilov E P, Nika D L and Balandin A A 2004 *J. Appl. Phys.* **95** 5626

[29] Komirenko S M, Kim K W, Stroscio M A and Dutta M 2000 *Phys. Rev.* B **61** 2034

[30] Lü J T and Cao J C 2005 *J. Appl. Phys.* **97** 033502

[31] Wood C and Jena D 2008 *Polarization Effects in Semiconductors* (New York: Springer) pp. 42–56

[32] Tuchman J A and Herman I P 1992 *Phys. Rev.* B **45** 11929

[33] Guo X G, Tan Z Y, Cao J C and Liu H C 2009 *Appl. Phys. Lett.* **94** 201101

[34] Wu J Q 2009 *J. Appl. Phys.* **106** 011101